together with those of fish, turtle, crocodile and frog (Table 1), well-rounded pebbles and concretions and haphazardly oriented molluscan shells. The nature and the extent of breakage, wearing and abrasion observed on the skeletal parts indicate a scatological origin. A comparison of the proportional percentage representation with skeletal elements in some of the Pleistocene microvertebrate accumulations[14] suggests that the present microvertebrate remains might have been transported, sorted and finally deposited fluvially in a stream channel area. Large vertebrate fauna (in addition to those mentioned earlier, *Panthera leo*, *Panthera tigris*, *Panthera pardus* (?), *Canis aureus*, *Rhinoceros* sp., *Stegodon insignis ganesa*, *Elephas namadicus*, *Hexaprotodon namadicus*, *Sus* sp., *Antilope cervicapra*, *Cervus* sp., *Axis axis*, etc.) indicates the presence of open grasslands and wooded grasslands interspersed with perennial rivers and swamps[8]. Since most of the taxa in the present collection of microvertebrates closely resemble the living forms, the preliminary interpretations of palaeoecology are based on the principle of actualism. Rodents like *Tatera indica* and *Gerbillus indus* prefer sandy plains and interdunal areas[18]. African *Tatera* is found primarily in dry steppic countries and sometimes in thickets along the edges of alluvial flats[19, 20]. *Bandicota bengalensis* and *Millardia meltada* are found in croplands where the sub-soil moisture is very high throughout the year. The latter sometimes prefer heavy shrubs and rocky terrains[21]. *Cyprinus*, *Crocodylus*, *Trionyx* and *Rana* are commonly associated with freshwater stream systems.

Tatera indica, *Gerbillus indus*, *Bandicota bengalensis* and *Millardia meltada* are presently widespread all over the Indian subcontinent[22]. The molars of *Tatera* cf. *T. indica* and *Gerbillus* sp. (Figure 2 *d, e*) resemble those of *Protatera* cf. *P. kabulense* reported from Late Pliocene of Siwaliks. *Bandicota* cf. *B. bengalensis* and *Millardia* cf. *M. meltada* (Figure 2 *a–c*) may have had some relationships with *Bandicota sivalensis* and cf. *Millardia*[23] from Upper Siwaliks. However, keeping in view the relatively meagre record of fossil micromammals, interrelationship of Narmada and Siwalik rodents cannot be ascertained at the present state of our knowledge.

1. Theobald, W., *Mem Geol. Surv. India*, 1860, **2**, 279–298.
2. Terra, H. de and Paterson, T., *Carnegie Instn Washington Publ*, 1939, **493**, 313–326.
3. Badam, G. L. and Salahuddin, *Curr. Sci*, 1982, **51**, 898–899.
4. Pilgrim, G. E., *Rec. Geol. Surv. India*, 1905, **32**
5. Sonakia, A., *Rec Geol Surv India*, 1984, **113**, 159–172.
6. Kennedy, Kenneth A. R., Sonakia, A., Chiment, John and Verma, K. K., *Am J. Phys Anthropol.*, 1991, **86**
7. Badam, G L., Ganjoo, R K. and Salahuddin, *Palaeogeogr. Palaeoclimatol. Palaeoecol.*, 1986, **53**, 335–348.
8. Badam, G. L., *Deccan College PGRI Pune Publ.*, 1979, 167–184
9. Agrawal, D P. and Kusumgar, S., *Prehistoric Chronology and Radiocarbon Dating in India*, Munshiram Manoharlal, New Delhi, 1974, p. 41.
10. Joshi, R V. and Kshirsagar, A., *Deccan College PGRI Pune Publ.*, 1986
11. Agrawal, D P., Kotlia, B. S. and Kusumgar, S., *Proc Indian Nat Sci Acad*, Part A, 1988, 418–424
12. Grigson, C., *Recent Advances in Indo-Pacific Prehistory*, Oxford & IBH Publ, New Delhi, 1985, pp 425–428.
13. Mellett, J. S., *Science*, 1974, **185**, 349–350.
14. Korth, W. W., *Ann Carnegie Museum*, 1979, **48**, 235–285
15. Andrews, P. and Evans, E. M. N., *Paleobiology*, 1983, **9**, 289–307.
16. Wolff, R. G, *Palaeogeogr Palaeogeoclimatol Palaeoecol*, 1973, **13**, 91–101.
17. Dodson, P. and Wexlar, D., *Paleobiology*, 1979, **5**, 275–284.
18. Prakash, I. P. and Ghosh, P. K, Dr W. Junk B V. Publishers, The Hague, 1975, pp 75–114
19. Coe, M, *J. Geogr.*, 1972, **138**, 316–338.
20. Hubert, B, *Bull. Carnegie Museum Nat Hist*, 1978, **6**, 109–112.
21. Prater, S T. L., *The Book of Indian Animals*, Bombay Natural History Society, Bombay, 1971, pp. 1–324
22. Roberts, T. J., *Mammals of Pakistan*, Ernest Benn, London & Tonbridge, 1977, pp. 218–304.
23. Patnaik, R., Unpublished Ph D Thesis, Panjab University, Chandigarh, 1993, pp. 1–158
24. Badam, G. L. and Grigson, C., *Modern Geol*, 1990, **15**, 49–58.

ACKNOWLEDGEMENTS. We thank IGRMS, Bhopal, for the financial support. RP thanks CSIR, New Delhi, and DAAD, Bonn, for funding a part of the research. Dr P. S. Joshi and Sri S. A. Pradhan provided the technical help.

Received 10 February 1994, revised accepted 23 January 1995

Daytime measurements of optical auroral emissions from Antarctica

R. Sridharan, D. Pallam Raju, R. Narayanan, N. K. Modi, B. H. Subbaraya and R. Raghavarao

Physical Research Laboratory, Ahmedabad 380 009, India

Optical methods have enabled us to detect auroral emissions during daytime conditions, and to identify a narrow latitudinal region of energetic particle precipitation from the Indian station Maitri (11°38'E; 70°45'S; 62.8°S I-lat.) in Antarctica. These observations are new. The energetic particles originate within the closed geomagnetic field lines close to the plasmapause region and maximize ~0830 h MLT (Magnetic Local Time) (~1200 UT). Enhanced proton precipitation activity could also be inferred during a moderate geomagnetic storm, suggesting the enhancement/activation of acceleration mechanisms during this event.

THE auroral phenomenon, which is caused by the interaction of high-energy charged particles with the atmospheric constituents is usually considered to be restricted to ±75° to ±80° magnetic latitudes in the dayside and ±65° to ±75° magnetic latitudes in the nightside of the earth. Due to the different locations of the geomagnetic

and the geographic poles, the region of maximum occurrence probability of aurora is in the form of an oval and this is usually referred to as the auroral oval. In the dayside, where the solar wind kinetic pressure distorts the dipole-like configuration of the geomagnetic field, a narrow region around 80° south and north geomag. lat., referred to as the cusp, gets connected to the interplanetary space. The solar wind particles would then be directly guided into this region while the ionospheric particles would freely escape into the interplanetary medium. In the dayside, the polar cusp is the only region that maintains direct contact with the solar wind plasma. From magnetic topology point of view the cusp gets mapped into the dayside magnetopause region. From the available information in the literature, mostly based on rocket and satellite measurements, it is known that the dayside precipitation in the cusp region is less energetic compared to the nighttime conditions and as a consequence the emissions would preferably occur at higher heights (~150 km and above as compared to 110–120 km during nighttime). Significant amount of atomic emissions are known to occur due to lesser collisional deactivation at higher altitudes. There are no systematic ground-based observations on the variabilities of the optical signatures of aurora during daytime till now, mainly because of the inherent difficulty in the detection and measurement of these faint features in the presence of bright background continuum. The only attempt, a pioneering one, to detect daytime auroral emissions was made by Noxon[1] from the high-latitude regions in the northern hemisphere using a scanning polarimeter. Though successful detection of these emissions was made from the conventional auroral zone, no systematic intensity measurements could be made because of the inherent limitation in the technique.

In recent years, a new method has been used at PRL for the detection of faint emission features which constitute only 0.1% of the bright background continuum[2]. This new method has been used for the measurement of airglow emissions during daytime clear-sky conditions and several new results have already been obtained from equatorial and low-latitude regions[3–5].

The limitation of the dayglow photometer of being able to monitor only one wavelength at a time has been overcome by the use of innovative spiral masks[6]. These appropriate changes in the optics and introduction of electronic gate scanning techniques have enabled near simultaneous measurements of three emissions at different wavelengths. A specially coated (3900–8000 Å) Fabry–Perot etalon has been used as a narrow-band spatial filter. The details of the measurement techniques would be presented elsewhere.

The choice of the filters was made so as to represent the high- and low-energy electron-excited as well as proton-excited emissions. The multiwavelength daytime photometer was operated in a meridional scanning mode pointing towards magnetic south, the look angles ranging from 10° elevation to zenith in steps. The look angle, the choice of filters and appropriate gate delays were programmed to be automatically selected by a personal computer. The meridional scans, once in three minutes, were repeated round the clock. The information obtained represents the intensity variation of the chosen wavelengths with time. Observations were made at N_2^+ 1Neg. bands at 3914, 4278 and 4709 Å (high-energy electron-excited), OI 5577 Å (low-energy electron-excited) and 4861 Å H_β (proton-excited) emissions. Figure 1 depicts the surface plots of the variations in intensities with time and invariant geomagnetic latitude on two days, viz. 6 Feb. and 19 Feb. 1994. The various latitudes have been estimated based on the typical altitude of emission and the look angles, for three wavelengths.

The most striking observation is a steep rise in intensities at all the three wavelengths, namely 4709 Å, 4861 Å and 5577 Å at around noon hours (UT). The enhanced intensities are confined to a narrow latitudinal zone centred around 64°S mag. lat. and extend by ~2° in latitude. Large wave activities are seen to be centred around the peak emission and the associated particle precipitation. Unlike the other emissions, the 5577 Å emission is centred at 63°S. The background variation of 5577 Å emission is considerably lesser than its noontime peak. These observations indicate that the region of 5577 Å emission is narrower while the high-energy electron-excited and proton-excited emissions have a larger spatial spread. The present observations could be visualized as follows. The regions of particle precipitation and excited emissions are geomagnetically controlled and are expected to have a fixed orientation with respect to the sun. Due to the separation between the geographic and geomagnetic poles and the consequent precession of the magnetic pole with respect to the axis of rotation, the observational site cuts through the region of deposition around noon. This could result in the type of observed variations.

On 6 Feb., when the magnetic disturbance level was moderate, ($\Sigma K_p = 43-$), the overall intensity levels were found to be higher than that on 19 Feb. ($\Sigma K_p = 31$) and also on other days when the level of magnetic activity was considerably lower. Further, beyond 68°S mag. lat. no enhancement in the emissions is seen. The boundary at 68°S and the level of wave activity are depicted in Figure 2, wherein the two-dimensional ground projection of 4861 Å (proton-excited) intensities on 4 days during the month of February are shown along with the magnetic activity level (ΣK_p). The curves represent constant-intensity contours. As mentioned earlier, the latitudinal extent of the emission region is confined to 64° ± 1°S. Further, it is clearly seen that the wave activity associated with peak emission/deposition of energetic particles is quite prominent. During magnetically

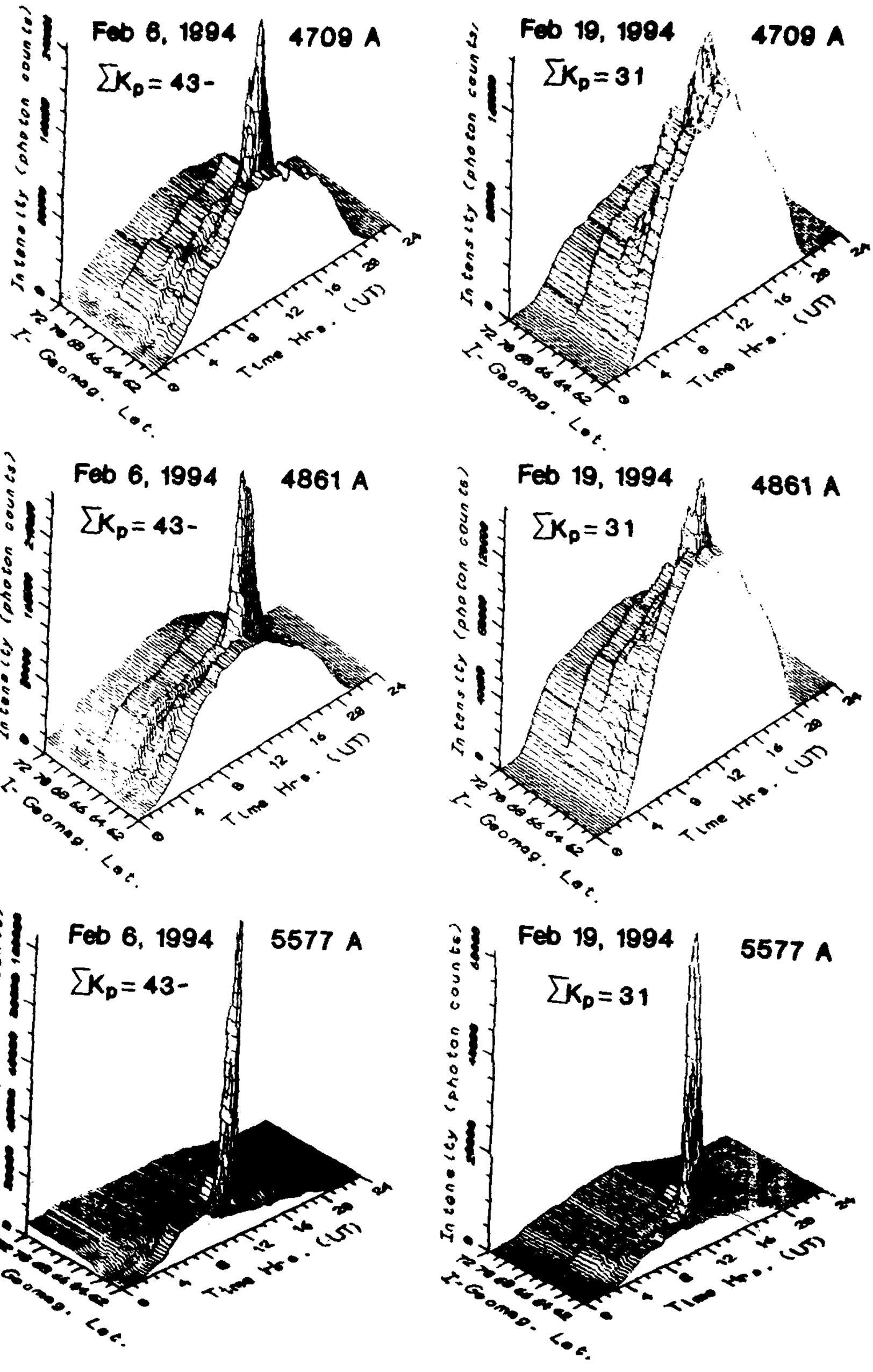

Figure 1. The temporal and latitudinal variabilities in the high-energy electron-excited (4709 Å), in proton-excited (4861 Å) and in low-energy electron-excited (5577 Å) daytime auroral emissions as recorded at Maitri – the Indian station at Antarctica – on 6 and 19 Feb 1994.

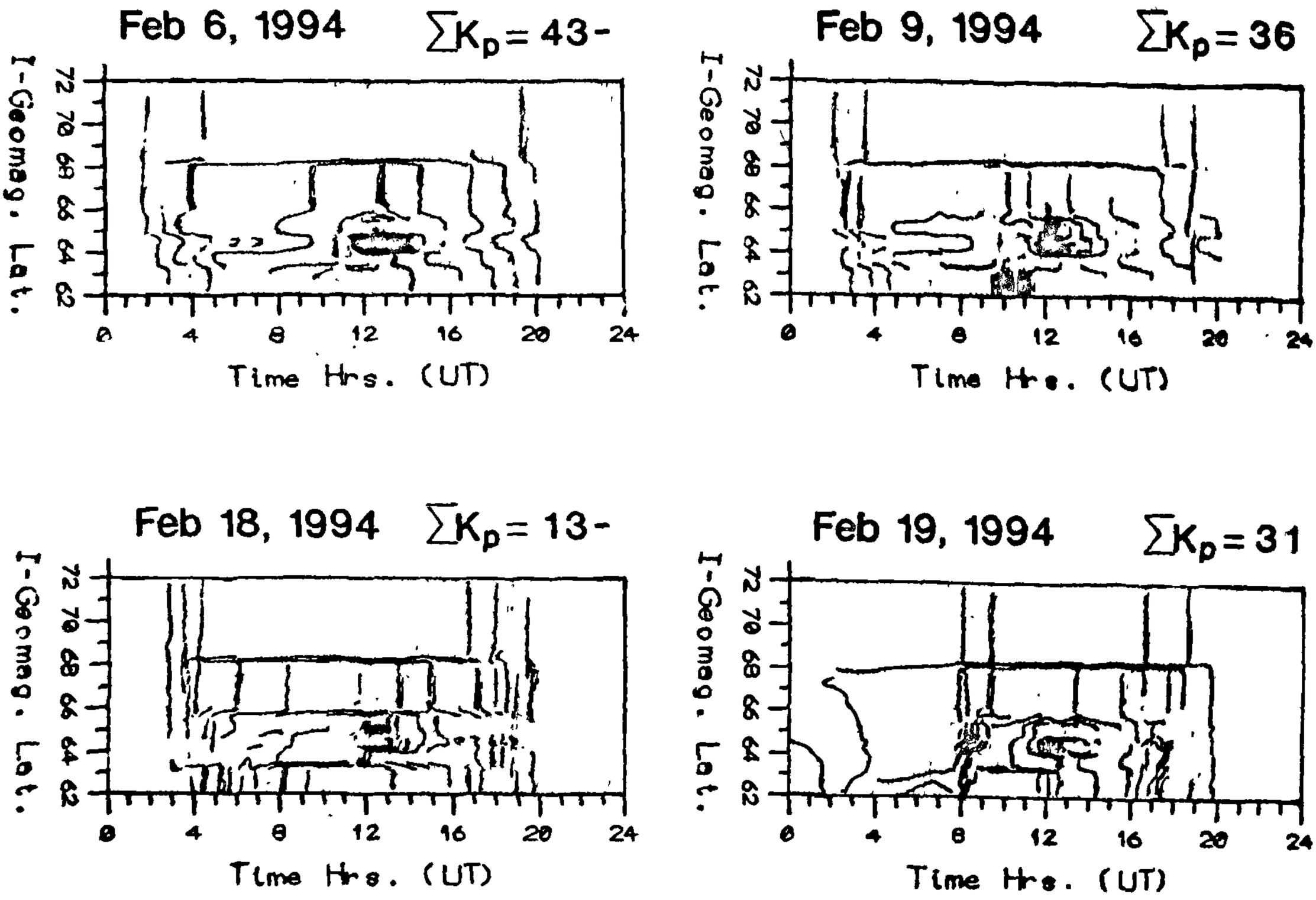

Figure 2. Ground projections of 4861 Å intensities during magnetically quiet and disturbed periods depicting the wave activity in the constant-intensity contours

quiet periods the wave activity is found to be low. Figure 2 shows the extent to which the activities are localized.

Though there have been no ground-based daytime optical measurements till now, it has been reported from the analysis of satellite data that there exists a region of particle precipitation in the ±60° to ±70° mag. lat., maximizing around 0630–1000 MLT[7]. Hartz[7] suggested that this rise in intensity in the forenoon hours could be due to the upper atmosphere acting as a sink for the particles in the outer Van-Allen belt region. Nighttime photometric measurements by Samson *et al.*[8] have also revealed narrow and sharply defined latitudinal zones of auroral emissions associated with electron and ion precipitations. Newell *et al.*[9] have attempted to classify regions of auroral activity based on satellite data and have mentioned the latitude zone of our interest to be possibly excited by particles originating from the central plasma sheet. VLF and ELF emissions have also been shown to maximize in this latitude zone around 0830–1030 MLT[10]. Through this communication, we are providing evidence, for the first time, from ground-based optical measurements for the presence of a narrow latitudinal zone of enhanced auroral activity in the daylit side of the earth. Incidentally, the L value of the Indian Antarctic station Maitri being 4.8, the geomagnetic field line passing through this station crosses the plasmapause – a critical transition region between the plasmasphere and the magnetosphere during the afternoon hours. The plasmapause is defined as the boundary between the magnetic flux tubes that corotate with the earth and those whose motion is dominated by the convective electric fields. Since the plasmapause is a sharply-defined region, elongated in the dusk sector[11],

depending upon the solar wind ram pressure and the local time, the field lines over Maitri can be mapped either to the outer boundary of the plasmasphere or to the inner boundary of the magnetosphere. This makes it a unique location. Further, the enhanced intensities during a geomagnetic storm are a clear indication of a certain acceleration mechanism becoming more active during such events. A detailed investigation of the origin of the particles and their possible acceleration mechanism is in progress.

The present conclusions have been arrived at from the data collected on 13 clear days from Antarctica during January–February 1994 as a part of the XIIIth Indian Scientific Expedition. More extensive campaigns are being planned during the ensuing southern summer months.

1 Noxon, J F , *J Atmos Terr Phys* , 1963, **25**, 637–645
2 Narayanan, R , Desai, J. N , Modi, N K., Raghavarao, R and Sridharan, R , *Appl Optics*, 1989, **28**, 2138–2142.
3 Sridharan, R , Raghavarao, R , Gurubaran, S. and Narayanan, R , *J Atmos Terr Phys* , 1991, **53**, 521–528
4 Sridharan, R., Haider, S. A , Gurubaran, S , Sekar, R. and Narayanan, R , *J Geophys Res* , 1992, **97**, 13715–13721
5 Sridharan, R., Pallam Raju, D , Raghavarao, R and Ramarao, P V. S , to appear in *Geophys Res Lett* , 1994
6 Sridharan, R , Narayanan, R , Modi, N. K and Pallam Raju, D , *Appl Optics*, 1993, **32**, 4178–4180
7 Hartz, T R , *Particle Precipitation Patterns in the Radiating Atmosphere* (ed Mc Cormac, B. M), Reidel, Dordrecht, 1971, pp 225–238
8 Samson, J C , Lyons, L. R., Newell P T , Creutzberg, F and Xu, B , *Geophys Res Lett* , 1992, **19**, 2167–2170
9 Newell, P T , Patrick, T. and Ching, I. Meng , *J Geophys Res* , 1994, **99**, 273–286
10 Barrington, R E. and Palmer, F. H , in *Magnetosphere–Ionosphere Interactions* (ed. Folkestad, K.), Proc. of the Advanced Study Institute, Norway, 1971, pp 97–104.
11 Sharp, G W., Chappell, C. R and Harris, K K., in *Magnetosphere–Ionosphere Interactions* (ed. Folkestad, K), Proc of the Advanced Study Institute, Norway, 1971, pp 169–183

ACKNOWLEDGEMENTS The logistic support for the above study was provided by the Department of Ocean Development (DOD), Government of India This work is supported by the Department of Space (DOS), Government of India Our thanks are due to Prof R K. Varma, Director, PRL, for his keen interest and constant encouragement We duly acknowledge the assistance given by Mrs Vijaya Mutagi in the fabrication of the instrument.

Received 5 December 1994, revised accepted 7 February 1995

Complexation and interaction modelling in a thorium(IV) – mycobacterial-siderophore system

H. J. MacCordick, O. Wendling and M.-S. Antony

Centre de Recherches Nucleaires et Université Louis Pasteur, Laboratoire de Chimie Nucléaire, F-67037 Strasbourg Cedex 02, France

Assessment of the role of bacterial cell components in the biosorption of actinide cations involves studies of the metal ion complexing properties of siderophores. In the present work, the interaction of thorium ions with mycobactin S from *Mycobacterium smegmatis* is examined *in vitro*, as a model system, using ethanol as the solvent medium. Formation of a labile addition compound is followed by UV spectrophotometry, which reveals characteristic absorption in the 330 nm region. Hydrolytic dissociation measurements with the ^{228}Th-labelled complex at pH 7 indicate lower stability than for the corresponding uranyl–mycobactin compound under analogous conditions. The properties of the thorium complex are rationalized by calculations of metal–ligand bond character and steric relationships at the molecular binding site.

APPLICATIONS of microorganisms and microbial constituents as complexing agents in the treatment of radwaste are finding widespread interest[1–3]. Previous work with a mycobacterial species has shown that this substrate is effective in the selective biosorption and retention of various actinide cations such as Th^{4+} and UO_2^{2+} or Am^{3+} on a Eu^{3+} carrier[3,4]. Measurements based on NMR and infrared spectroscopy applied to cellular extracts and model compounds have confirmed that the adsorption process involves cation interaction with specific cell components containing acidic functional groups such as those in phospholipids and non-esterified carboxylate[5].

The possible contribution of the mycobacterial siderophore in this respect has been tested with purified

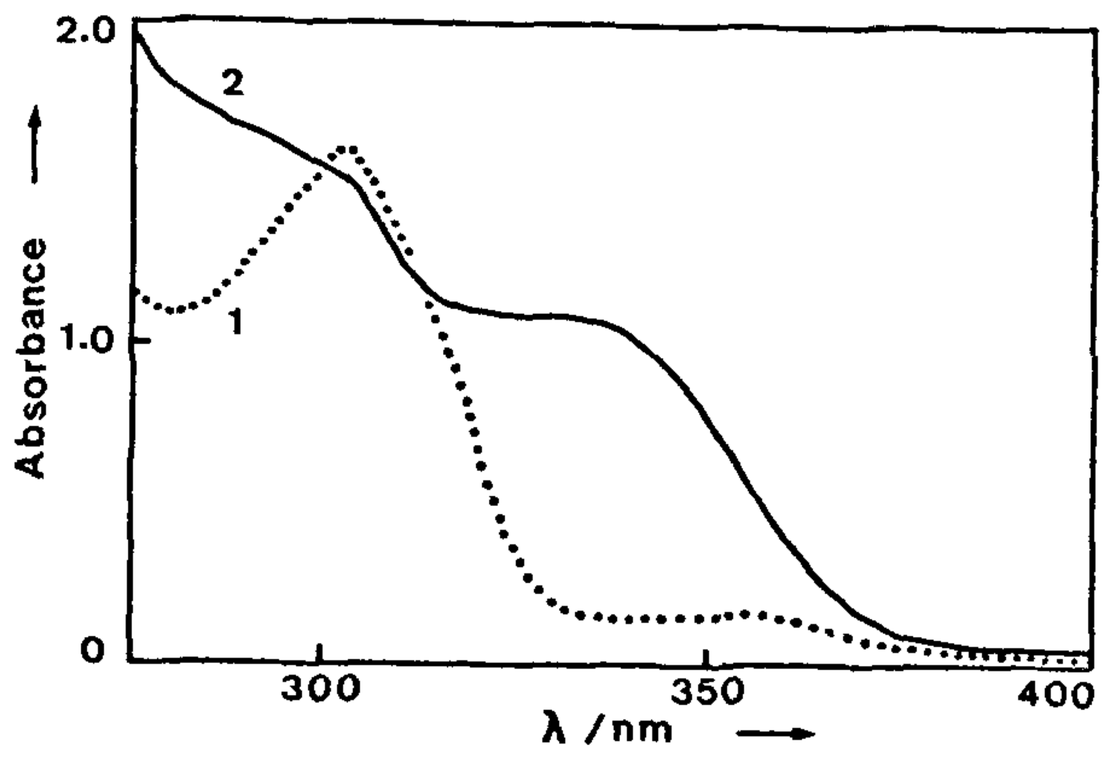

Figure 1. UV absorption spectra for MYS (•••, 1) and Th–MYS (——, 2) in ethanol